Design and measurements of a broadband two-dimensional acoustic lens

Lucian Zigoneanu, Bogdan-Ioan Popa, and Steven A. Cummer[*]

Department of Electrical and Computer Engineering, Duke University, Durham, North Carolina 27708, USA
(Received 4 March 2011; published 26 July 2011)

We describe the design, fabrication, and measurement of a 2D broadband gradient index acoustic lens in air. The index of refraction is tuned by controlling the dimensions of acoustic metamaterial unit cell inclusions designed through numerical simulations. The lens was fabricated in plastic through rapid prototyping stereolithography, and measurements of the sound field show good agreement with the theoretical lens performance. The broadband performance of the lens is confirmed for frequencies ranging from 1.5 kHz to 4.5 kHz.

PACS number(s): 42.79.Ry, 46.40.Cd, 43.20.El, 43.20.Bi

I. INTRODUCTION

A gradient index medium (GRIN) is a medium in which the index of refraction or sound speed varies. This property and the consequent applications have been widely investigated over the last three decades for optical frequencies.[1] Recent advances in acoustic metamaterials have made the control of the index of refraction profile more precise and its variations limits much broader. Therefore, the realization of GRIN media for acoustic waves has become more practical. For example, it has been analytically shown that a periodic structure formed from solid cylinders placed in a fluid or gaseous background could act as a homogeneous medium, with specific effective parameters controlled by the filing ratio.[2–4]

Acoustic media in which the refractive index varies continuously in a direction perpendicular to the optical axis can focus sound. Although the focus could be realized using negative refractive index (for example, see Ref. [5]), the operating frequency range for this lens is small. Also, because the lattice parameter should be comparable with the wavelength, the final product will be very large for low frequencies. A different approach[6] relies on controlling how the index of refraction varies along the axis transverse to the direction of propagation using periodic structures, and for simple inclusion geometries analytical expressions between the effective material parameters and the filling ratio (i.e., the lattice parameter) could be obtained. Acoustic lenses based on this method have been experimentally demonstrated for air and water background, respectively.[7,8]

Here, we describe and apply a different, numerical design method for acoustic GRIN lenses with some advantages over previous approaches, including higher refractive index, lighter weight, and better impedance matching. We build on a numerical approach[9,10] to design unit cells with specific acoustic effective material parameters, and then fabricate via stereolithographic rapid prototyping an array of different unit cells to create the desired index of refraction profile. Measurements of the resulting sound field are in good agreement with simulated predictions and confirm the broadband performance of the lens.

II. LENS AND METAMATERIAL DESIGN

We want to create an index of refraction n which has a hyperbolic secant variation in the direction perpendicular to the propagation direction (Fig. 1). This profile for the index of refraction is capable of focusing acoustic waves with no aberrations.[4] Our aim is to have a maximum value for n as large as possible such that for the same focal length the lens will be as thin as possible. For our design and fabrication approach, the largest value for the index of refraction that can be realized is close to 2, as we will see later. However, this value leads to a focal length suitable for measurement in our experimental setup and to a thinner lens than previously reported designs.[7] From the index of refraction curve, we select the ideal values corresponding to the position of the center of the unit cell and we create unit cells with an index of refraction that closely match these values.

The unit cell was designed using air as background fluid and for a frequency of 3 kHz (11.43 cm wavelength). The final design will be 2.0 wavelengths wide in the transverse direction and 0.31 wavelengths long in the propagation direction. The position of the focal point along the acoustic axis analytically predicted by ray theory[1,7] is 10.13 cm. This distance is measured from the edge of the lens. The complicated relationship between lens thickness and maximum index for a fixed focal length[1,7] means that there is not a precise relationship between maximum index and lens thickness. However, for the parameter range of our lens and that described in Ref. [7], we find that the thickness is approximately proportional to $n_{\max}^{-2.2}$, meaning that our $n_{\max}$ of 2 yields a lens that is approximately 2.5 times thinner than previous designs.[7]

So that the entire structure of unit cells behaves like an isotropic acoustic metamaterial, we choose a unit cell dimension approximately 10 times smaller than the operating wavelength [Fig. 2(a)]. This is sufficiently small that the effects of the spatial structure on the effective properties of the metamaterial are modest.[9] The form of the unit cell is a solid cross placed in air (background fluid). The cross design is an effective one for keeping the impedance Z of the unit cell close to the background medium. It was previously shown[9] that for a unit cell of this kind the effective density (thus, n) is controlled by the size of the gaps between consecutive solid inclusions, and the effective bulk modulus (thus, Z) is controlled by the volume fraction of the solid relative to the background.[3,11] A cross structure enables small gaps, and thus high effective densities, while keeping the total volume fraction of the solid to a minimum, thus keeping the effective bulk modulus close to that of air. Since $Z = nB$ and the desired index of refraction is fixed as in Fig. 1, the unit cell impedance will be minimized if the bulk modulus of the unit cell is the smallest possible.
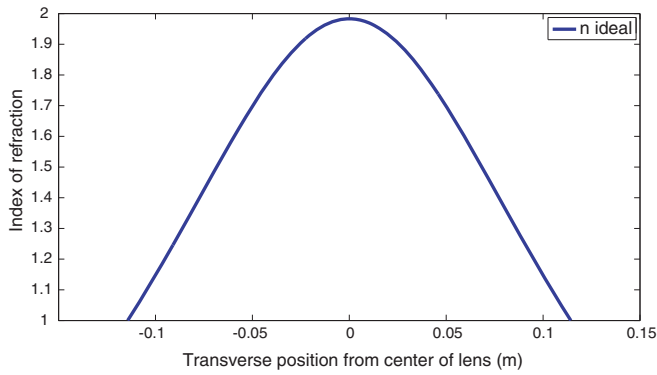
FIG. 1. (Color online) Desired index of refraction along the direction transverse to propagation direction.

For example, a unit cell consisting of a square with $2a$ side placed in air background will have a higher effective acoustic impedance than the same unit cell formed from a cross with dimensions a and b placed in air background.

The design goal is to vary the dimensions a and b of the cross such that we obtain the desired index of refraction and the minimum mismatch between the impedance of the surrounding fluid and the impedance of the unit cell, respectively. There are certain practical limitations. The largest value of a (hence the smallest gap) must be such that the unit cells can be fabricated with the stereolithographic approach, and the smallest value of b (hence the thinnest solid structure) must be chosen such that the final structure is stable and not prone to buckling or collapsing under its own weight. A maximum value for a of 5.7 mm (or a 0.6 mm gap) and a smallest value for b of 1 mm can be easily realized in practice. Having the constraints explained above, we keep $b = 1$ mm fixed for all unit cells (i.e., to have the minimum impedance

possible for the unit cell) and tune n by varying the dimension a [Fig. 2(b)]. The largest value for $n = 1.98$ is obtained for $a = 5.7$ mm.

Although the refractive index of a material could be analytically computed for a periodic structure regardless of the geometry, for example see Ref. 13, we decided to find the effective parameters of a given unit cell through a numerical simulation, using the procedure described in Ref. 9, because it is relatively easy to apply and has been previously confirmed in both theory and experiment that this method is correct. A brief summary of this procedure follows. A pressure plane wave is excited with normal incidence onto a single unit cell in a domain with periodic boundary conditions on the transverse edges of the domain, in order to simulate a transversely infinite array of unit cells [Fig. 2(c)]. The reflection and transmission coefficients (amplitude and phase) are computed and then inverted in order to obtain the index of refraction and effective impedance of the unit cell.[12] The values for the index of refraction n and impedance Z for the unit cells that will be used are presented in Fig. 3. We show only the positive values of the transverse position from the center of the lens, as the lens is symmetric about its center.

As the a dimension increases, both n and Z increase. With our design, for the n specified in Fig. 1, the largest impedance mismatch is 2.6 (i.e., the impedance of the unit cell in the center of the lens is 2.6 times larger than that of the air). This yields an impedance contrast between the lens and air that is approximately two times smaller than previous designs.[3,7] A key advantage of this design method is that it can be easily applied for any shape of the solid inclusion. It has been shown that other inclusion shapes can produce a greater index of refraction without a significant change to the effective bulk modulus.[9] The current design was sufficient for our goals and could be easily fabricated without any major challenges.
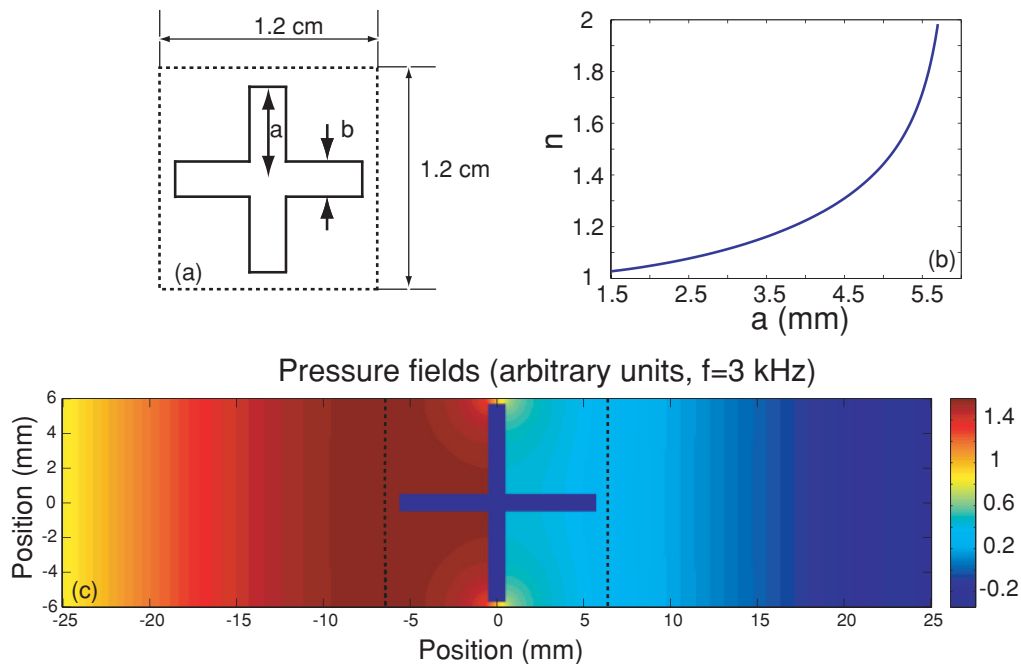
FIG. 2. (Color online) (a) Unit cell dimensions. (b) Index of refraction vs a dimension of the cross. (c) Simulations for acoustic wave propagation ($f = 3$ kHz).
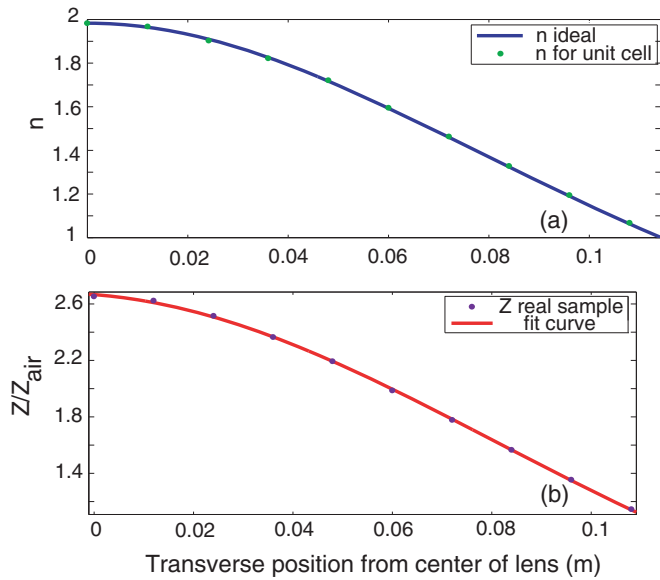
FIG. 3. (Color online) (a) Index of refraction along the direction transverse to the propagation direction (desired and realized in practice). (b) Unit cells' impedance and their position on the axis perpendicular to propagation direction.

To validate the design and make sure that the discretization in unit cells will act as expected, we performed two additional simulations using the Acoustic-Structure Interaction Module of COMSOL MULTIPHYSICS: one for the entire structure of unit cells (the actual lens) and one where we replaced the lens with a continuous, lenslike domain in which the index of refraction varies continuously as in Fig. 1 and the impedance varies continuously as in Fig. 3(b) (fit line). The material parameters used in simulations for the crosses are the same as the material parameters of the crosses realized in practice. Both simulations were performed for a waveguide that has the dimensions of the actual waveguide where we realized the experiment and

that is bordered by perfectly matched layers. A pressure wave from a point source is propagating from left to right and the pressure field inside the waveguide is computed. As can be seen in Fig. 4, the acoustic metamaterial realization of the lens performs virtually exactly like the idealized smoothly inhomogeneous lens material properties. This validates the design and shows that good lens performance can be obtained with a fairly simple acoustic metamaterial design.

III. LENS FABRICATION AND CHARACTERIZATION

The final lens design was drafted using AutoCAD and was fabricated using stereolithography with the DSM Somos ® 9420 Photopolymer (density ≈ 1.13 g/cm^3 at room temperature, Poisson's ratio 0.43, and modulus of elasticity 553–850 MPa) and a finish that yielded a final product with the designed dimensions. The individual crosses were built upward from a 1 mm thick plate which was used to anchor the cross-shaped pillars. A photograph of the fabricated lens is shown in Fig. 5(a).

The lens performance was investigated by measuring the spatial variation of the sound field in a 1.2 m^2 parallel plate waveguide. The distance between the 0.5 cm thick ABS plastic plates is 5.08 cm, which gives a cutoff frequency of 3.38 kHz. A 3 inch diameter speaker was used to generate a pulsed signal that travels through the waveguide. The exact shape of the pulse and its characteristics are described in detail in Ref. 10. It consists of a Gaussian-modulated pulse with 5 wave periods of the fundamental frequency. The resulting pulse is compact in time so that the incident and reflected pulses do not overlap and can be easily processed, and relatively narrow in bandwidth (30% bandwidth) so that the measurements probe the lens performance at nearly a single frequency.

Two signals are measured at two locations in the waveguide using two preamplified condenser microphones. One microphone was placed in a fixed position close to the speaker and was used as a time reference. The other microphone was
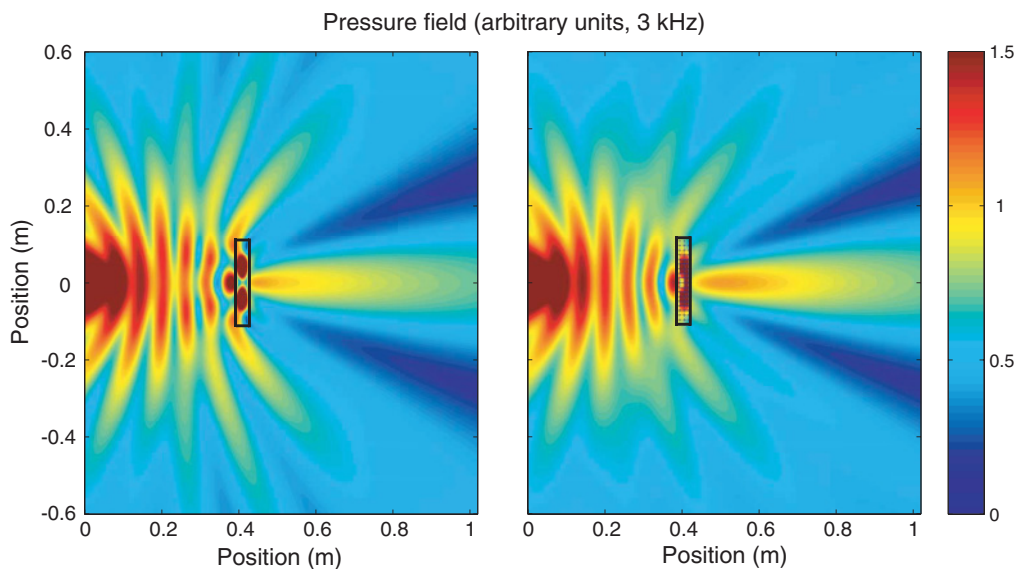
FIG. 4. (Color online) Comparison between simulated sound fields for an idealized lens with continuous material parameters (left) and the actual structured lens (right). The good agreement confirms the suitability for realizing the lens with a metamaterial approach.
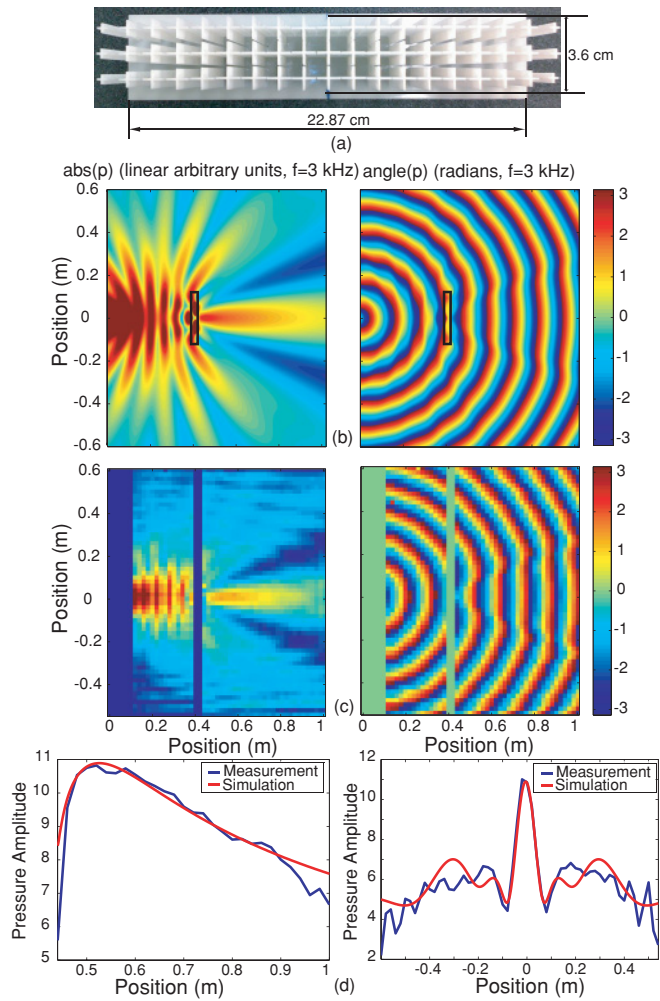
FIG. 5. (Color online) (a) The actual lens. (b) Simulated pressure field amplitude (left) and phase (right) for continuous lens domain. (c) Measured pressure field amplitude (left) and phase (right). (d) Pressure amplitude (arbitrary units) on a line passing through the focal point in the propagation direction (left) and in a direction transverse on the propagation direction (right).

FIG. 6. (Color online) (a) Simulated pressure fields for the entire domain (left) and measured/simulated pressure amplitude slices through focal point and far away from the focal point at 4.5 kHz (right). (b) Simulated pressure fields for the entire domain (left) and measured/simulated pressure amplitude slices through focal point and far away from the focal point at 1.5 kHz (right).

scanned inside the waveguide, using a stepper motor, and measured the pressure field throughout the waveguide. The measurement points were placed in a square grid of 2 cm to provide at least 4 measurement points per wavelength. The signals from the two microphones were sampled by a National Instruments data acquisition card. For an increased signal to noise ratio, several measurements are made and averaged for each measurement point. No scans are made along the lines where the lens is present because the apparatus does not allow the microphone to be placed there.

First, we investigated the lens at the designed frequency (3 kHz). We align in time all the signals collected by the microphone moving inside the waveguide using the reference signals to ensure a common phase reference. Then, we isolate the incident and first reflection pulses from other reflections (e.g., reflections from the edges of the waveguide) and use the Fourier transform to determine the amplitude and phase of the signal. This procedure yields some artifacts for measurement points that are extremely close to the edges of the waveguide,

where the second reflection overlaps over the useful portion of the signal. However, excellent agreement between simulation and measurements is observed for both amplitude and phase of the total pressure field. The results are presented in Fig. 5 and they clearly show the focusing effect and the focal distance, which closely match the focal distance predicted by ray theory. Due to our experimental setup, we were unable to have measurement points very close to the speaker and along the lens position. From the comprehensive set of simulations and measurements presented in Figs. 5(b) and 5(c), we extracted two relevant lines going through the focal point in the propagation direction and in a direction transverse to the propagation direction, respectively. Then, we plotted the pressure profiles along these two lines in order to furthermore highlight the lens behavior of our structure [Fig. 5(d)].

Second, we investigated the broadband properties of our lens. There are some limitations in exploring this property. As we decrease the frequency from 3 kHz, the dimension of the lens in the transverse direction will become smaller compared

with the wavelength and the focusing property will diminish. On the other hand, as we increase the frequency over 3 kHz, the unit cell will become larger compared with the wavelength and eventually the effective medium homogenization concept will not apply to this material. However, we were able to confirm the focusing properties of the lens as low as 1.5 kHz and as high as 4.5 kHz, as shown in Fig. 6. We performed simulations for the entire domain and extracted two relevant lines perpendicular on the propagation direction: through the focal point and far away after the focal point [see Fig. 6 (left column)] in order to highlight the pressure field maximums and minimums. Then, we performed measurements for these lines and compared them with the simulation results [Fig. 6 (right column)]. A good agreement between the experimental and the expected results is observed. As can be seen, the agreement is better at 4.5 kHz, where the unit cell dimension is approximately six times smaller than the wavelength and the homogenization still takes place. At 1.5 kHz the lens dimension is only one wavelength in the transverse direction and thus the focusing effect is weakest and hard to accurately detect with our apparatus and processing technique. Moreover, as the frequency decreases (larger wavelength), the reflections from the edge of the waveguide are harder to remove. We should note that although over 3.4 kHz there is another propagating mode present in the waveguide, it has a group velocity much lower than the first mode and does not influence our processing technique.

IV. CONCLUSIONS

A method for the design, fabrication, and measurement of a 2D broadband gradient index acoustic lens in air is presented. The lens was designed using an acoustic metamaterial approach that employed a numerical technique to tune the effective refractive index with position in the lens. Simulations confirmed that the physical structured lens performance matched that of the ideal materials. The lens was fabricated via stereolithographic rapid prototyping, and measurements of the resulting sound field confirmed the good performance of the lens and the correctness of the design. The resulting lens is lighter and thinner than related GRIN lenses previously reported in the literature because of the design and fabrication technique employed. The broadband performance of the lens was also experimentally demonstrated by measurements from 1.5 kHz to 4.5 kHz.

ACKNOWLEDGMENTS

[*] cummer@ee.duke.edu

[1] C. Gomez-Reino, C. Bao, and M. V. Perez, *Gradient Index Optics: Fundamentals and Applications* (Springer, Berlin, 2002).

[2] D. Torrent, A. Hakansson, F. Cervera, and J. Sánchez-Dehesa, Phys. Rev. Lett. **96**, 204302 (2006).

[3] D. Torrent and J. Sánchez-Dehesa, Phys. Rev. B **74**, 224305 (2006).

[4] S.-C. S. Lin, T. J. Huang, J.-H. Sun, and T.-T. Wu, Phys. Rev. B **79**, 094302 (2009).

[5] S. S. Peng, Z. J. He, H. Jia, A. Q. Zhang, C. Y. Qiu, M. Z. Ke, and Z. Y. Liu, Appl. Phys. Lett. **96**, 263502 (2010).

[6] D. Torrent and J. Sánchez-Dehesa, New J. Phys. **9**, 323 (2007).

[7] A. Climente, D. Torrent, and J. Sánchez-Dehesa, Appl. Phys. Lett. **97**, 104103 (2010).

[8] T. P. Martin, M. Nicholas, G. J. Orris, L. W. Cai, D. Torrent, and J. Sánchez-Dehesa, Appl. Phys. Lett. **97**, 113503 (2010).

[9] B. I. Popa and S. A. Cummer, Phys. Rev. B **80**, 174303 (2009).

[10] L. Zigoneanu, B. I. Popa, A. Starr, and S. A. Cummer, J. Appl. Phys. **109**, 054906 (2011).

[11] A. B. Wood, *A Textbook of Sound; Being an Account of the Physics of Vibrations with Special Reference to Recent Theoretical and Technical Developments* (Macmillan, NewYork, 1955).

[12] V. Fokin, M. Ambati, C. Sun, and X. Zhang, Phys. Rev. B **76**, 144302 (2007).

[13] A. A. Krokhin, J. Arriaga, and L. N. Gumen, Phys. Rev. Lett. **91**, 264302 (2003).